



SPE 99325

The Impact of Interfacial Tension and Pore Size Distribution/Capillary Pressure Character on CO₂ Relative Permeability at Reservoir Conditions in CO₂-Brine Systems

Brant Bennion, Hycal Energy Research Laboratories Ltd., Calgary, AB, Canada, and
Stefan Bachu, Alberta Energy and Utilities Board, Edmonton, AB, Canada

Copyright 2006, SPE

This paper was prepared for presentation at the 2006 SPE/DOE Symposium on Improved Oil Recovery held in Tulsa, Oklahoma, U.S.A., 22–26 April 2006.

This paper was selected for presentation by an SPE Program Committee following review of information contained in an abstract submitted by the author(s). Contents of the paper, as presented, have not been reviewed by the Society of Petroleum Engineers and are subject to correction by the author(s). The material, as presented, does not necessarily reflect any position of the Society of Petroleum Engineers, its officers, or members. Papers presented at SPE meetings are subject to publication review by Editorial Committees of the Society of Petroleum Engineers. Electronic reproduction, distribution, or storage of any part of this paper for commercial purposes without the written consent of the Society of Petroleum Engineers is prohibited. Permission to reproduce in print is restricted to an abstract of not more than 300 words; illustrations may not be copied. The abstract must contain conspicuous acknowledgment of where and by whom the paper was presented. Write Librarian, SPE, P.O. Box 833836, Richardson, TX 75083-3836, U.S.A., fax 01-972-952-9435.

Abstract

Injection of CO₂ has been used for enhanced oil recovery (EOR) in many light and medium gravity reservoirs. Consequently, sequestration of CO₂ in oil reservoirs in conjunction with CO₂-EOR is a method that is under consideration for reducing CO₂ emissions into the atmosphere. Many oil reservoirs are underlain by an aquifer, and EOR processes often involve water-alternating-gas (WAG) processes. Proper understanding of the relative permeability character of such systems is essential in ascertaining CO₂ injectivity and migration, and in assessing the suitability and safety of prospective CO₂ injection and sequestration sites. While many measurements exist for CO₂-oil systems, very few data, if any, exist for CO₂-brine systems.

This paper provides an analysis of brine-CO₂ interfacial tension (IFT) measurements that were conducted for equilibrium brines and CO₂ at reservoir conditions, and the detailed 700 MPa mercury-injection capillary pressure tests conducted on all rock samples to determine specific pore size distributions. Three sandstone and three carbonate potential sequestration zones in the Wabamun Lake area in Alberta, Canada, were evaluated, together with a caprock shale. This data set has specific application to the study of the behavior of injected CO₂ in contact with bottom water or water saturated zones that may be encountered in CO₂-EOR projects, as well as for CO₂ sequestration in deep saline aquifers. The analysis shows some correlation between the CO₂-brine IFT, the pore size distribution of the intercrystalline porous media and the CO₂-brine relative permeability character. However, due to the high degree of variability in the pore system character of the different sandstone and carbonate facies tested, additional,

better-controlled comparative tests are required to validate these trends. The hope is that, ultimately, the compilation of these more extensive enhanced datasets will allow appropriate selection of proper CO₂-brine relative permeability relationships at reservoir conditions for intercrystalline sandstone and carbonate formations on the basis of relatively simple measurements of pore system geometry and IFT. These data will also provide a valuable tool for the estimation of CO₂-brine relative permeability for the simulation and evaluation of intercrystalline sandstone and carbonate formations on a worldwide basis.

Introduction

Enhanced oil recovery (EOR) is being used to increase the recovery of oil from oil reservoirs beyond their natural production by injecting water (secondary recovery) and/or gases or solvents (tertiary recovery). Carbon dioxide is being used for tertiary EOR in more than 70 operations in the United States, the great majority of them being located in the Permian basin in west Texas¹. The main reason for the successful development of this industry is the availability of low-cost CO₂ from the huge McElmo Dome, St. Johns and Jackson Dome natural CO₂ reservoirs in Colorado, Arizona and Mississippi, respectively, which together produce more than 18 MtCO₂/year (980 MMcfd)². Other CO₂-EOR operations in the U.S. and around the world use CO₂ from anthropogenic sources such as gas plants and petrochemical and fertilizer plants. However, very few CO₂-EOR operations exist outside U.S. because of the high cost of CO₂. In Canada, a large CO₂-EOR operation at Weyburn in southeastern Saskatchewan uses ~1 MtCO₂/year that is pipelined from the North Dakota Coal Gasification Plant in Beulah, N.D., while a much smaller operation at Joffre in Alberta uses CO₂ produced at a nearby petrochemical plant. Currently, natural gas, nitrogen and NGL-enriched natural gas are used for tertiary recovery in Alberta at more than 70 operations because they have historically been less expensive than CO₂. However, spurred by the potential of CO₂ geological storage as a climate change mitigation strategy³, and more specifically by the promise of CO₂-EOR as a low-cost or even profit-making option^{3, 4}, several oil producers in Alberta started in 2005 CO₂-EOR pilot operations using CO₂ from gas plants, and discussions are

currently ongoing about constructing a backbone CO₂ pipeline that will carry CO₂ produced at oil sands plants in northeastern Alberta to major oil fields in central and west-central Alberta that are currently undergoing secondary or tertiary recovery. In all these operations, the injected CO₂ will come in contact with formation water, yet very few data are available about the behavior of CO₂-brine systems, as most of the research effort to date has focused on CO₂-oil systems.

The need for data regarding relative permeability, interfacial tension (IFT) and capillary pressure of CO₂-brine systems has increased recently as a result of existing and planned operations for injecting into deep saline aquifers the CO₂ that is produced as a result of processing natural gas to bring it to market specifications. For example, since 1995 Statoil is injecting ~1 MtCO₂/year into the Utsira aquifer at 800 m below the sea bottom at Sleipner in the North Sea, and is in an advanced stage of design for a similar operation in the Barents Sea. BP started injecting in 2004 a similar amount of CO₂ at 1800 m depth at In Salah in Algeria. There the CO₂ is typically injected into the aquifer that underlies the gas reservoirs that are the source of CO₂. Similar operations planned by Chevron at Gorgon Island in offshore northwestern Australia are in an advanced stage of design and regulatory review. Injection of CO₂ into deep saline aquifers will increase significantly during the first half of the 21st century because they have the greatest capacity for CO₂ geological storage, which is one option in a portfolio of actions for reducing atmospheric emissions of anthropogenic CO₂^{3, 5}. In both cases of CO₂ injection, into oil reservoirs or into deep saline aquifers, there is need for reliable data because both the flow of CO₂ and the storage of CO₂ as an immobile phase in the pore space at irreducible saturation⁶ depend on the capillary pressure, interfacial tension and relative-permeability of the CO₂-brine-rock system.

To cover this gap in data and knowledge, the authors undertook in 2004 a series of tests on core plugs taken from three sandstone, a shale and three carbonate formations in the Wabamun Lake area southwest of Edmonton in Alberta, western Canada. Multiple samples were taken from several of the formations providing four distinct sandstone, one shale and five carbonate data sets. The relative permeability results for CO₂ displacing brine (drainage) were reported previously⁷, and the capillary pressure and IFT results are presented in this paper. These results are most likely representative for subsurface conditions in sedimentary basins onshore North America between the Appalachians and Rocky Mountains that underwent similar cycles of deposition, compaction and erosion, but probably they are not representative for weakly compacted or uncompact basins like the North Sea and Gulf of Mexico, where permeability and porosity are much higher. Because this paper is basically the second in a series of three papers, the reader is referred to the previous paper⁷ for details regarding the geological setting and location of the wells with core samples used for measurements. Suffice to say that two sandstone and the three carbonate formations are host to many oil and gas reservoirs in Alberta.

The specific details of the equipment and procedures used to conduct the relative permeability measurements and the corresponding results have been presented by the authors in the previous paper⁷ for seven sets of rock samples from three sandstone and three carbonate formations (two sets, with low and high permeability, were analyzed and presented there for the carbonate Wabamun Group). Results specific to the work presented here include the high-pressure air-mercury capillary pressure measurements and the interfacial tension (IFT) measurements at reservoir conditions for the same seven sets, plus measurements for an additional data set each for the sandstone Viking Formation and carbonate Nisku Formation, and a data set for the Calmar Formation shale. Thus, ten sets of rock samples were analyzed in total. On the other hand, relative permeability and IFT were measured on the high-permeability Wabamun sample set for three different conditions⁷: 1) in-situ pressure, temperature and brine salinity, 2) low pressure and temperature (same salinity), and 3) freshwater at in-situ temperature and pressure, to assess the effects of these three variables on the parameters of interest. The new Viking and Nisku rock samples were tested at the same in-situ conditions of temperature, pressure and brine salinity as the corresponding Viking and Nisku samples in the original sets, to assess the effect of rock properties. This brings to twelve the number of relative permeability measurements, but with only nine corresponding IFT measurements.

Laboratory Measurements

The capillary pressure measurements were conducted using a computerized 400 MPa Micromuretics air-brine capillary pressure apparatus. This technique has been well established in the industry and is discussed in numerous technical papers⁸. Sample rock chips of approx 2.5 cm diameter were taken from the endcap sections of the plugs that were tested for relative permeability, to provide samples as representative as possible of the actual porous medium being tested. Mercury is used to represent the non wetting phase, while the mercury vapor phase represents the wetting phase in the reservoir. Highly accurate capacitance measurements are used to evaluate the exact volume of mercury injected into the sample as a function of applied pressure, to generate the mercury injection capillary pressure curve. Since the IFT and contact angle of mercury and air are known (485 dynes/cm and approximately 130 degrees, respectively) it is possible to derive from these data the specific pore throat size distribution of the sample being tested and the porosity fraction of the sample that is accessed by these specific pore throat diameters. In addition, the mercury injection data can be used to construct an air-mercury capillary pressure curve. If the reservoir-condition contact angle for a gas-brine system and the gas-brine IFT is known, it is possible to convert the air-mercury data back to appropriate reservoir conditions using the relationship:

$$\frac{P_{C-RF}}{P_{C-Hg-air}} = \frac{\sigma_{RF} \cos(\theta_{RF})}{\sigma_{Hg-air} ABS[\cos(\theta_{Hg-air})]}$$

Reservoir-condition IFT measurements between the injected CO₂ and the formation brine are required for a proper conversion of the data. It is essential that these fluids are in thermodynamic equilibrium in order to obtain a stable IFT. For this reason the reservoir brine and CO₂ were precontacted with each other at reservoir temperature and pressure conditions and shaken until an equilibrium condition of saturation had been established between the two phases. The phases were then separated maintaining a constant temperature and pressure and charged into a high pressure and temperature drop-pendant IFT cell. Figure 1 provides a schematic illustration of this apparatus. A droplet of equilibrium brine, surrounded by the equilibrium gas, is suspended at bottomhole temperature and pressure conditions from the tip of the small bore capillary tube which extended into the optically visible portion of the sight cell, and a digital high magnification image of the configuration of this drop is obtained. The drop image is shown on a digital monitor and updated twice every second. When the drop matures, the profile is digitally captured and extracted in a file. An optimization software package is used to match the surface curvature of the drop with the solution of the Laplace equation for the solution of the IFT. A detailed description of this method is contained in the literature⁹.

Experimental Results

Pore Characteristics

Table 1 provides a summary of the pore characteristics, capillary pressure and permeability to brine at in-situ conditions for the ten samples that were evaluated in the study. The minimum initial pressure level for mercury intrusion on the apparatus is 3.5 kPa. Samples that exhibit this low threshold pressure typically contain large exposed surface dissolution pores and/or exposed vugular porosity. Specific information regarding fraction of micropores (<1 micron diameter pore throats), mesopores (1-3 microns diameter pore throats) and macropores (>3 micron pore throat diameters) is of interest, as well as the median (average) pore throat diameter and threshold intrusion pressure representing the pressure required in order to first push mercury into the largest pores present in the sample. Figure 2 presents the pore throat size distributions for these samples and Figure 3 provides the corresponding converted CO₂-brine capillary pressure curves for reservoir-conditions.

As expected, the shape of the capillary pressure curves reflects pore size distributions (e.g., see Figures 3c, 3g and 3b and the corresponding uni-, bi- and tri-modal pore size distributions in Figures 2c, 2g and 2b; or the jagged capillary pressure in Figure 3g that corresponds to the absence of pores of certain sizes in the Nisku sample of Figure 2g). Also as expected, the threshold pressure decreases with increasing pore size (see the pairs for Viking and Wabamun in Figures 2a-3a and 2e-3e, respectively; or compare the Basal Cambrian sandstone and Calmar shale, Figures 2c-3c and 2d-3d, respectively). The tri-modal pore size distribution of the Ellerslie Fm. (Figure 2b) is likely due to the presence of leached porosity in clays and grains, as opposed to the cleaner sandstones of the Viking and

Basal Cambrian (Figures 2a and 2c, respectively). The carbonate rocks generally display more complex pore distributions (Figures 2e-2h) than the siliciclastics (Figures 2a-2d).

There is no correlation between porosity and pore size characteristics (fraction of micro-, meso- and macro-porosity, or median pore size), and this is not unexpected because porosity is a measure of the volume (amount) of pores, not of their size and distribution. On the other side, pore size and distribution affect the ability of fluids to pass through, and indeed reasonable correlations have been found between permeability to brine and median pore size (Figure 4) and also fraction of large pores. The data spread is due to both the broad set of rocks with large degree of variation in properties and structure, but also to the differences in pressure, temperature and salinity, which affect brine interfacial tension, density and viscosity. In addition, the interest was to determine if correlations exist between the CO₂ displacement character (represented by parameters such as the endpoint relative permeability to CO₂ and maximum CO₂ saturation) and pore characteristics (size, capillary pressure), but no such relationships were identified. If they exist, the large degree of variability in the in-situ conditions and the character of the different formations tested in this study did not allow their clear identification, however some general trends were observed in the data.

Interfacial Tension

Table 2 presents the results of interfacial tension measurements for the ten different conditions of pressure, temperature and salinity that were used in the study. The data indicate that pressure affects the strongest the IFT between brine and CO₂ (Figure 5), which has been observed previously for other fluid pairs and is an expected result. The trend is defined mostly by the two end members at low and high pressures, while the middle region shows rather the absence of a definite trend. At first glance, the data suggest also a dependence of IFT on temperature similar to the one on pressure (not shown), but this is most likely an artifact caused by the dependence of both in-situ pressure and temperature on sample depth, hence it is the likely result of the strong correlation between temperature and pressure.

However, temperature and salinity also affect IFT, although their effect is milder and more difficult to detect in the current set of experimental data, and these variations in temperature and salinity are most likely the cause of the lack of a definite trend for the middle region in Figure 5. A drop in salinity from 144,304 ppm to none results in an IFT reduction of only from 29.53 dyne/cm to 28.89 dyne/cm (cases 3 and 4 in Table 2), suggesting that, although brine salinity has an effect, this effect is likely small compared with pressure and temperature effects. Also, examination of cases 1 and 2 in Table 2 would suggest that IFT should be less for the Ellerslie conditions than for the Viking ones because of a pressure increase, but instead a slight increase in IFT is observed, which corresponds to a significant increase in both temperature and salinity. On the other hand, a similarly significant increase in salinity

between the Ellerslie and Wabamun in-situ conditions (cases 3 and 4) fails to lead to an increase in IFT when the increase in temperature is much smaller. Comparison of IFT for the Wabamun and Calmar in-situ conditions (cases 3 and 6) shows that the increase in pressure and a slight decrease in salinity had a stronger effect than the slight increase in temperature, but the comparison between the Calmar and Nisku results (cases 6 and 7) shows that the effect of a significant increase in pressure could not counteract the effects of a large increase in temperature and of a much smaller one in salinity that lead to an increase in IFT, contrary to expectations. Finally, it is worth noting that the IFT is almost the same, ~ 27 dyne/cm, for both Calmar and Basal Cambrian conditions (cases 6 and 9), although pressure is significantly higher for the latter than for the former, but so is temperature.

The previous analysis indicates that the IFT of CO₂-brine systems is strongly affected by pressure (with decreasing IFT with increasing pressure), but also by temperature, with an increase in IFT with increasing temperature. Salinity also has an effect, with increasing IFT as salinity increases, but this effect is significantly smaller. The temperature and salinity effects on IFT working against pressure effects are also intuitive when considering that CO₂ solubility in brine increases with pressure and decreases with increasing temperature and salinity. Thus, although a large body of previous work for other fluid systems seems to indicate that IFT for binary component systems with no inherent mutual solubility is only weakly impacted by temperature¹², the data here suggest that temperature has a stronger effect in the case of CO₂ and this may be due not only to solubility effects, but also to phase effects. At low pressure and temperature CO₂ is a gas, as in case 5 in Table 2, which registered the highest IFT in the entire set, while at all other tested conditions CO₂ is a dense supercritical fluid. Although the current data set is insufficient to develop quantitative relationships between IFT and in-situ conditions for CO₂-brine systems, they point directionally to important conclusions and identify the need for systematic measurements and analysis..

A strong correlation between IFT and endpoint relative permeability to CO₂ is not apparent due to the variance in rock types, however a trend is observed in the existing dataset towards lower endpoint relative permeability to CO₂ as the CO₂-brine interfacial tension is increased. Additional points in the higher IFT range would serve to better round out the data set, but supplementary measurements were not conducted in this portion of the study and are proposed as a portion of the ongoing work on this project. A less distinct correlation is present between maximum CO₂ saturation and IFT, once again likely due to the high degree of variability in the different rock samples that were evaluated in the study. As with the previous endpoint relative permeability correlation, a general trend towards a reduction in maximum CO₂ saturation as the interfacial tension increases is apparent.

Attempting to correlate pore throat diameter statistics with maximum gas saturation indicated no discernable trend in the data set tested. However, although a large scatter in the data is present, there appears to be a loose trend for reduced endpoint

relative permeability to CO₂ as the fraction of macropores in the rock increased (and conversely as microporosity decreased). This seems at first to be contrary to expectations, but in highly heterogeneous pore systems containing large amounts of macroporosity it appears that there is a greater tendency to channel, resulting in less uniform displacement in the pore system and, hence, reduced relative permeability, in contrast to the more uniform dispersed displacement that appears to occur in the systems more dominated by micropores. It should be remembered that this correlation refers to relative, not actual permeability. The macro pore dominated systems in all cases had higher effective permeability to brine and CO₂.

Conclusions

This paper has presented and summarized the pore size, capillary pressure and interfacial tension characteristics for ten different rock sets from a variety of siliciclastic (sandstone and shale) and carbonate formations in the Wabamun Lake area of central Alberta, Canada. The IFT measurements were performed for CO₂-brine systems at nine different reservoir conditions of pressure, temperature and salinity. This limited data sample allowed drawing the following preliminary observations:

1. Pore characteristics (distribution and size) affect permeability and the shape and values of capillary pressure curves. As expected, permeability increases and capillary pressure decreases with increasing pore size and fraction of macro-pores. There is no relationship between porosity and pore characteristics.
2. Measured CO₂-brine IFT appears to be a relatively strong decreasing function of increasing reservoir pressure.
3. Although masked in the available data set by the increase in both temperature and pressure with depth, it appears that the CO₂-brine IFT increases with increasing temperature, but this effect is not as strong as the decrease in IFT with increasing pressure.
4. Water salinity also affects CO₂-brine IFT, although its effect is smaller than that of either pressure or temperature, leading to increasing IFT with increasing salinity.
5. The effects of temperature and salinity on the IFT of CO₂-brine systems are likely due to CO₂ solubility and phase effects, but this hypothesis needs to be verified through a systematic program of laboratory measurements.
6. Endpoint relative permeability value to CO₂ gas appears to be related to IFT (and hence also to pressure) and was observed to generally decrease as IFT increases (when pressure decreases).
7. A less pronounced trend of increasing maximum CO₂ saturation (a measurement of reservoir storage capacity) with decreasing IFT (and hence with increasing pressure) was observed.

8. There appears to be a relationship between the fractions of macro and microporosity present in the pore system and the endpoint relative permeability value to CO₂. Samples with higher fractions of microporosity appear to have a more uniform displacement character and higher endpoint relative permeability values to CO₂, most likely due to a more uniform displacement character.
9. The trends in points 6-8 above are based on the analysis of a broad spectrum of samples of widely varying lithology, pore size distribution and pore morphology. More controlled studies are required in order to validate the general trends observed in the data.
10. No trend in maximum CO₂ saturation character with pore size was observed in the tested sample set – possibly due to the wide variation in rock types evaluated in the study.
11. The results suggest that, from a CO₂-storage capacity perspective, in general, deeper, higher pressure formations which have a more uniform porosity character provide more storage capacity for CO₂ based on the maximum obtainable saturation and effective CO₂ maximum relative permeability.

Acknowledgements

The authors wish to express appreciation to the Alberta Energy and Utilities Board for permission to present these data, and to Donna Leach and Dan Magee for their assistance in the preparation of the manuscript and figures.

Nomenclature

P_{C-RF} = Reservoir condition CO₂-Brine capillary pressure – kPaa

$P_{C-Hg-air}$ = Air-Mercury capillary pressure – kPaa

σ_{RF} = Reservoir condition CO₂-Brine IFT – dyne/cm (mN·m)

σ_{Hg-air} = Air-Mercury IFT – dyne/cm (mN·m)

θ_{RF} = Reservoir CO₂-Brine contact angle – degrees

θ_{Hg-air} = Air-Mercury contact angle – degrees

References

1. Moritis G., Special Report: Enhanced Oil Recovery-2002 worldwide EOR survey; *Oil and Gas Journal*, v. 100, no. 15, 43-47, Apr. 15, 2002.
2. Stevens, S.H., Natural CO₂ fields as analogs for geologic CO₂ storage; *Carbon Dioxide Capture for Storage in Deep Geologic Formations – Results from the CO₂ Capture Project*, Volume 2 (ed. S.M. Benson), Elsevier, 687-697, 2005.
3. International Energy Agency, *Prospects for CO₂ Capture and Storage*, IEA/OECD, Paris, France, 249 p., 2004.

4. Intergovernmental Panel on Climate Change, *IPCC Special Report on Carbon Dioxide Capture and Storage* (eds. B. Metz, O. Davidson, H.C. de Coninck, M. Loos and L.A. Mayer), Cambridge University Press, Cambridge, U.K., and New York, NY, U.S.A., 442 p., 2005.
5. Socolow, R.H., Can we bury global warming? *Scientific American*; v. 293, no. 1, 49-55, 2005.
6. Kumar, A., Noh, M., Pope, G.A., Sepehrnoori, K., Bryant, S., and Lake, L.W., Reservoir simulation of CO₂ storage in deep saline aquifers; Paper SPE 89343, 10 p., presented at the SPE/DOE Fourteenth Symposium on Improved Oil Recovery, Tulsa, OK, USA, April 17-21, 2004.
7. Bennion, B., and Bachu, S., Relative permeability characteristics for CO₂ displacing water in a variety of potential sequestration zones in the Western Canada Sedimentary Basin; Paper SPE 95547, 15 p., presented at the 2005 SPE Technical Conference and Exhibition, Dallas, TX, October 9-12, 2005.
8. Pickell, J.J., Swanson, B.F., Application of air-mercury and oil-air capillary pressure in the study of pore structure and fluid distribution; *SPE Journal*, v. 6, no. 1, 55-61, 1966.
9. del Rio, O.I., and Neumann, A.W., Axisymmetric drop shape analysis: computational methods for the measurement of interfacial properties from the shape and dimensions of pendant and sessile drops; *Journal of Colloidal International Science*, v. 196, 136-147, 1997.
10. Kohl, A.L., and Nielsen, R.B., *Gas Purification*, Gulf Publishing Company, Houston, TX, USA, 1395 p., 1997.
11. Enick, R.M., and Klara, S.M., CO₂ Solubility in water and brine under reservoir conditions; *Chemical Engineering Communications*, v. 90, 23-33, 1990.
12. *Handbook of Chemistry and Physics*, CRC Press, 56th edition, 1976, pp. F23-36.

ID	Formation	% Micro Porosity	% Meso Porosity	% Macro Porosity	Median Pore Size (microns)	Porosity (%)	Threshold Capillary Pressure (kPa)	Permeability to Brine (md)
a	Viking I	33.8	13.5	52.7	3.760	12.5	28.8	2.700
a	Viking II	27.6	7.6	64.8	10.763	19.8	3.5	21.72
b	Ellerslie	59.6	20.9	19.5	0.277	12.6	56.3	0.376
c	Basal Camb.	65.1	29.5	5.4	0.919	11.7	31.9	0.081
d	Calmar	100.	0	0	0.006	3.9	72,827.0	0.00000294
e	Wabamun I	11.1	11.8	77.1	8.760	14.8	493.6	0.018
e	Wabamun II	81.0	18.9	0.1	0.645	7.9	57.2	66.980
f	Cooking Lk.	11.9	5.1	83.0	15.860	9.9	11.1	65.300
g	Nisku I	54.0	3.1	42.9	0.066	9.7	58.0	45.920
h	Nisku II	33.2	18.8	48.0	4.327	10.4	3.5	21.020

Table 1 – Pore and permeability characteristics of the ten sets of rock samples from the Wabamun Lake area, Alberta, Canada. The sets are listed in order corresponding to Figures 1 and 2, and, for easy identification, with the figure id indicated in the first column.

No.	Formation	Pressure (MPa)	Temperature (°C)	Salinity (ppm)	IFT (dyne/cm)
1	Viking	8.60	35	28,286	32.12
2	Ellerslie	10.90	40	97,217	32.45
3	Wabamun in-situ	11.90	41	144,304	29.53
4	Wabamun – freshwater	11.90	41	0	28.89
5	Wabamun low P & T	3.50	20	144,304	49.24
6	Calmar	12.25	43	129,688	27.60
7	Nisku	17.40	56	136,817	34.56
8	Cooking Lake	15.50	55	233,417	35.74
9	Basal Cambrian	27.00	75	248,000	27.01

Table 2 – Interfacial tension for CO₂-brine systems at in-situ conditions characteristic of siliciclastic and carbonate rocks in the Wabamun Lake area, Alberta, Canada. The data are listed in descending stratigraphic order, which generally coincides with increasing depth, hence pressure and temperature. Although the Cooking Lake Fm. is stratigraphically below the Nisku Fm., the respective rock sample originates from a well located updip from the well where the Nisku Fm. sample was taken from, resulting in shallower depth, hence lower in-situ pressure and temperature.

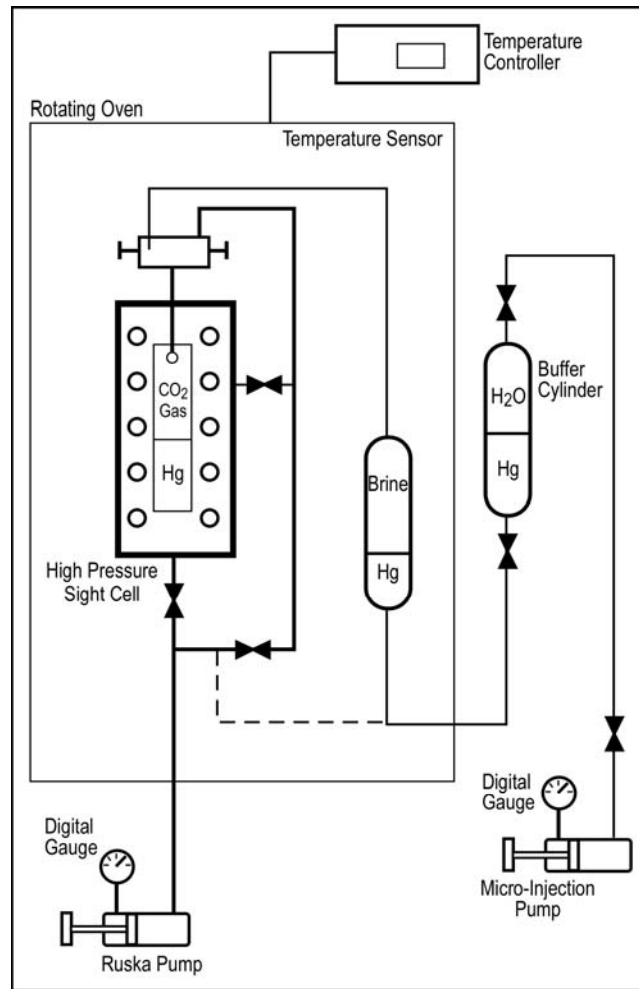


Figure 1 – Schematic diagram of the apparatus used for IFT measurements

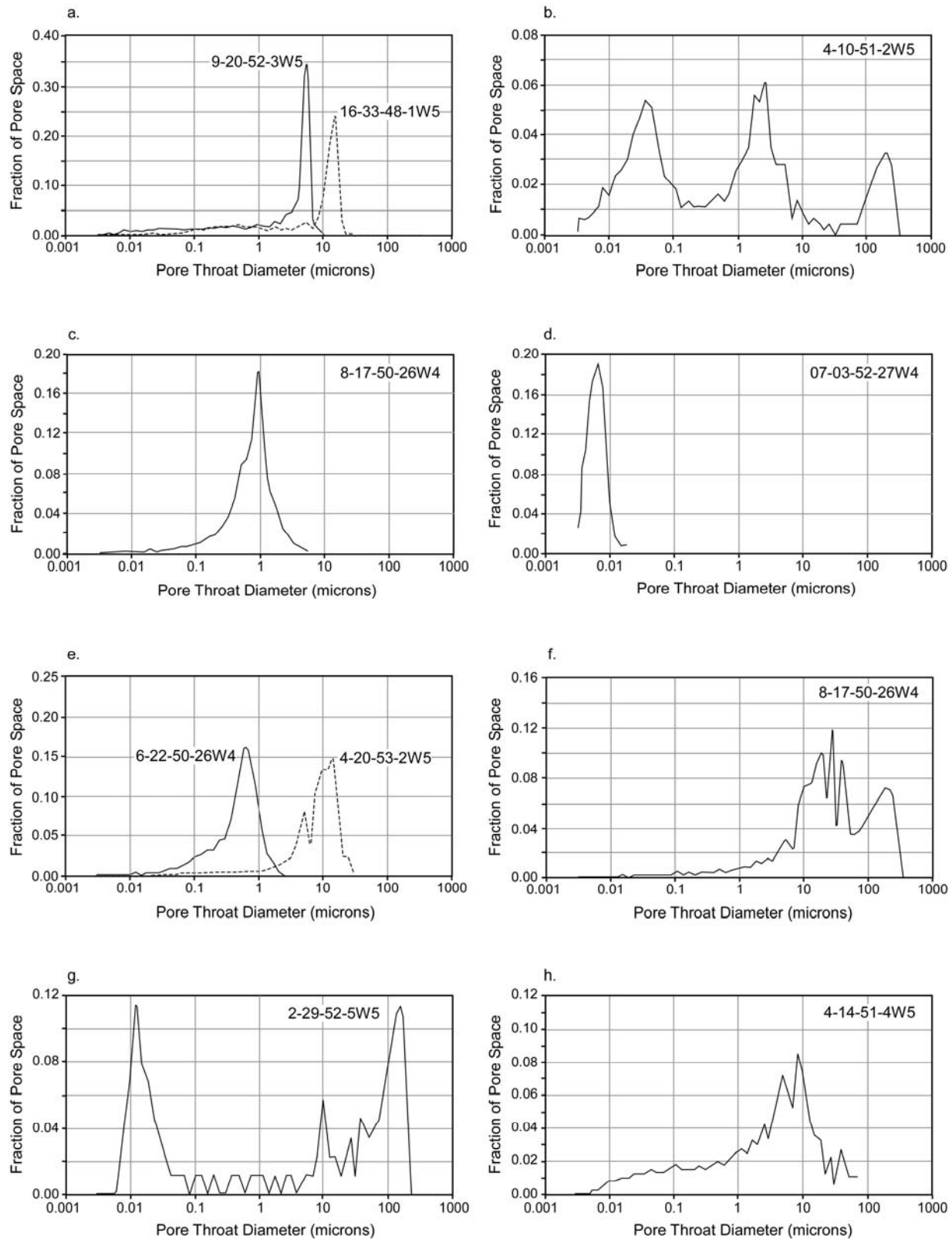


Figure 2 – Pore size distributions for the ten rock sample sets from the Wabamun Lake area, Alberta, Canada. The first three are for sandstones from the Viking (a), Ellerslie (b), and Basal Cambrian (c) formations, the fourth one is for the Calmar Fm. shale (d), and the last four are for carbonates of the Wabamun Group (e), Cooking Lake Fm. (f) and Nisku Fm. (g and h). The well location of each sample is indicated in the corresponding figure.

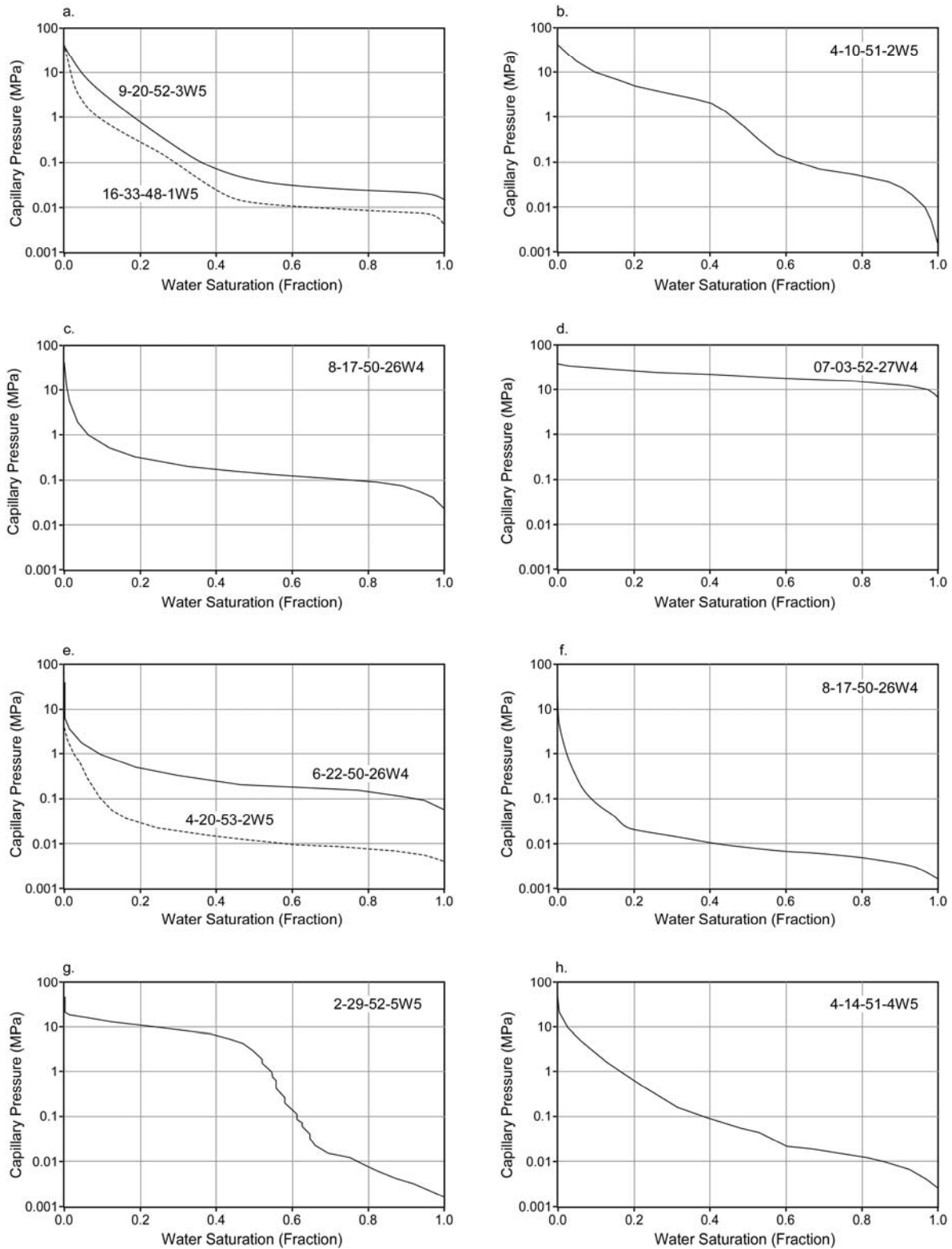


Figure 3 – Capillary pressure measurements for the ten rock sample sets from the Wabamun Lake area, Alberta, Canada. The first three are for sandstones from the Viking (a), Ellerslie (b), and Basal Cambrian (c) formations, the fourth one is for the Calmar Fm. shale (d), and the last four are for carbonates of the Wabamun Group (e), Cooking Lake Fm. (f) and Nisku Fm. (g and h). The well location of each sample is indicated in the corresponding figure.

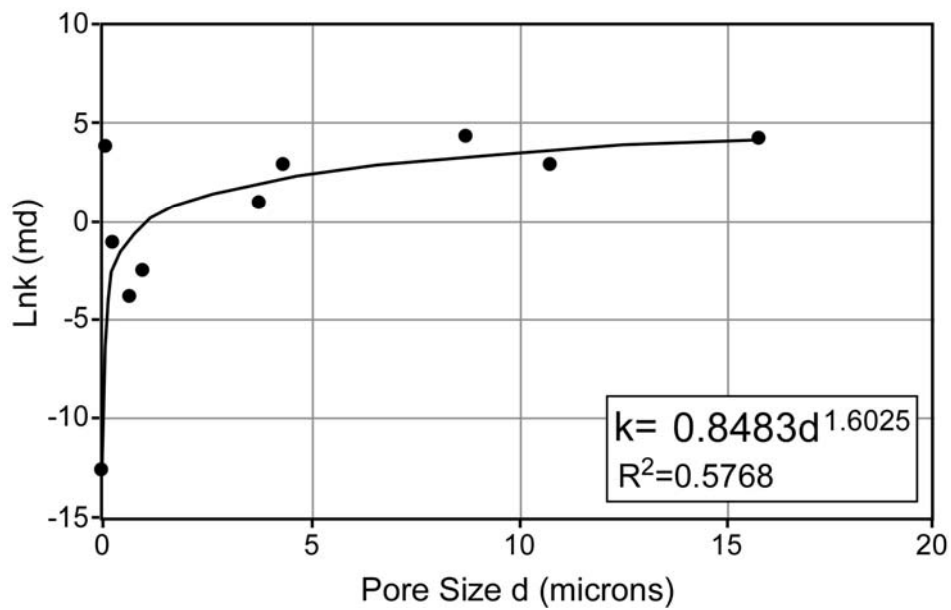


Figure 4 – Relation between permeability to brine at in-situ conditions and median pore size.

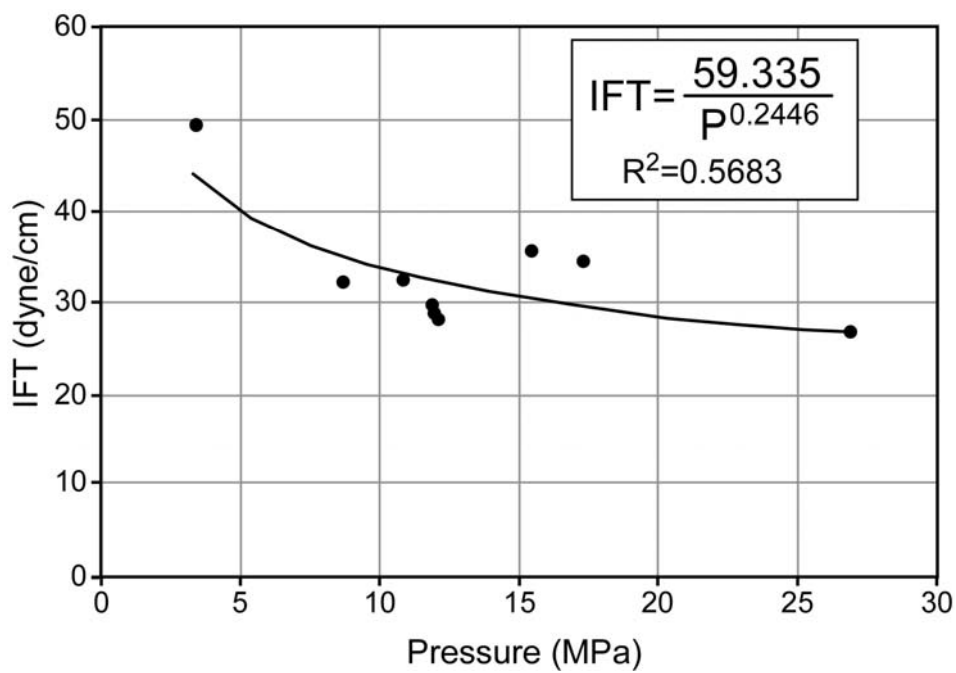


Figure 5 – Variation of interfacial tension for CO₂-brine systems with pressure.